AIMS Mathematics, 9(12): 36012–36030.
DOI: 10.3934/math.20241708
Received: 06 June 2024
Revised: 31 October 2024
Accepted: 03 December 2024
Published: 26 December 2024

https://www.aimspress.com/journal/Math

Research article

Representation of the solution of a nonlinear molecular beam epitaxy equation

Boubaker Smii*

King Fahd University of Petroleum and Minerals, Department of Mathematics, Interdisciplinary Research center for Intelligent Secure System, Dhahran 31261, Saudi Arabia

* **Correspondence:** Email: boubaker@kfupm.edu.sa.

Abstract: Stochastic partial differential equations (SPDEs) driven by Lévy noise are extensively employed across various domains such as physics, finance, and engineering to simulate systems experiencing random fluctuations. In this paper, we focus on a specific type of such SPDEs, namely the nonlinear beam epitaxy equation driven by Lévy noise. The Feynman graph formalism emerges as a potent tool for analyzing these SPDEs, particularly in computing their correlation functions, which are essential for understanding the moments of the solution. In this context, the solution to the SPDE and its truncated moments can be expressed as a sum over particular Feynman graphs. Each graph is evaluated according to a set of established rules, providing a systematic method to derive the properties of the solution. Moreover, the study delves into the behavior of the truncated moments for large times. Truncated moments, which capture the statistical properties of the system up to a certain order, are crucial for characterizing the long-term behavior and stability of the solution. The paper will conclude with a discussion on potential applications, highlighting the broader implications of this approach in various scientific and engineering contexts.

Keywords: SPDEs; Lévy noise; Green functions; Feynman graphs; truncated moments
Mathematics Subject Classification: 05C05, 60G20, 60H15

1. Introduction and overview

Molecular Beam Epitaxy (MBE) is a well known technology used to approach the essential research applied to the growth of semiconductor films and multilayer structures. Several works, see, e.g., [1, 2], are in one way or another connected with the nonlinear MBE universality class studied in [3, 4].

MBE is an ideal process used to create a crystalline structure. The term epitaxy refers to the deposition of an overlayer on a crystalline substrate. Whereas the term beam means that the evaporated elements, such as atoms and molecules, never interact with each other or with vacuum gases until they

impinge on the substrate.

MBE is more efficient and precise than other growth techniques primarily due to the reproducibility of all parameters during the epitaxial process and the ability to control the kinetic evolution of the epitaxial film layers. This advanced technology is widely used to produce lattice structures composed of multiple thin layers with extremely small thicknesses. MBE was invented and developed in the late 1960s at Bell Telephone Laboratories by J.R. Arthur and Alfred Cho, and has since become a groundbreaking and heavily researched technology for depositing single crystals.

In this work we consider a more general model for MBE given by the nonlinear stochastic partial differential equation (SPDE):

$$\begin{cases} \dfrac{\partial u}{\partial t}(t,\mathbf{x}) = -m\,\nabla^2 u(t,\mathbf{x}) - c\nabla^4 u(t,\mathbf{x}) + \beta\,\nabla^2|\nabla u(t,\mathbf{x})|^p + \xi(t,\mathbf{x}), \\ u(0,\mathbf{x}) = \phi(\mathbf{x})\ ;\ (t,\mathbf{x}) \in \Xi =]0,+\infty[\times L_\delta,\ \ m,\, c,\, \beta > 0, \end{cases} \tag{1.1}$$

where $L_\delta = \Big\{\delta z\ :\ \delta > 0,\ z \in \mathbb{Z}^d\Big\}$ is the lattice on $\mathbb{Z}^d$, $d > 0$.

The stochastic force $\xi(t,\mathbf{x})$ is a general space-time white noise of Lévy type that models height fluctuation due to the random deposition of materials, and ϕ is a given initial function. The constant m is associated with *surface diffusion*.

The term $-m\nabla^2 u(t,\mathbf{x})$ models the relaxation of surface height due to atomic diffusion along the surface. It describes how atoms tend to move to minimize surface energy and smooth out surface irregularities. However, the constant c is related to *surface tension* or *surface stiffness*.

The term $-c\nabla^4 u(t,\mathbf{x})$ models the effect of higher-order surface tension, which further smooths out the surface by penalizing sharp curvature changes. It acts as a stabilizing factor against surface roughness. Whereas the constant β controls the *nonlinear effects* during the growth process, the term $\beta\,\nabla^2|\nabla u(t,\mathbf{x})|^p$ represents nonlinear interactions in the surface morphology, where the parameter p defines the degree of nonlinearity. This term models how local changes in surface slopes affect the growth dynamics, potentially amplifying certain surface patterns.

Together, these constants influence the growth dynamics, surface smoothness, and pattern formation during the epitaxial process.

Stochastic differential equations (SDEs) driven by Gaussian noise have been intensively studied, and their solutions are well-documented (see, e.g., [5–8]). However, stochastic partial differential equations (SPDEs) of the form (1), which model a general MBE, are less explored, particularly with restrictions on the terms on the right-hand side of the equation. Relevant studies with such restrictions include [9–13]. Let us mention that to the best of our knowledge, this is the first study extending the previous class to nonlinear SPDEs driven by Lévy-type noise. (The extension should be understood in the sense that random variables with a Lévy distribution extended Gaussian random variables).

In the general model for the MBE given by Eq (1.1), ∇u is the discrete gradient defined by

$$\nabla u(\mathbf{x}) = \delta^{-1}\Big(u(\mathbf{x}+\delta\mathbf{e}_1) - u(\mathbf{x}), \ldots, u(\mathbf{x}+\delta\mathbf{e}_d) - u(\mathbf{x})\Big), \tag{1.2}$$

while the p-discrete gradient $\nabla^p u$ is defined as $\nabla^p = \nabla(\nabla^{p-1}u)$. If p is even, this is nothing else than the discrete $p-$Laplacian, and the Laplacian is defined by

$$\Delta u(\mathbf{x}) = \delta^{-2}\Big(-2d\,u(\mathbf{x}) + \sum_{|\mathbf{y}-\mathbf{x}|=\delta} u(\mathbf{y})\Big), \tag{1.3}$$

where $(\mathbf{e}_1, \cdots, \mathbf{e}_d)$ is the canonical basis of $\mathbf{R}^d$.

The main idea in this paper is to solve the SDPE (1.1) perturbatively by expressing the solution u as follows:

$$u(t, \mathbf{x}) = \sum_{i=0}^{\infty} (-\beta)^i u_i(t, \mathbf{x}). \tag{1.4}$$

To address the complexity of finding an analytic solution for the SPDE (1.1) in the form of power series, we introduce the Feynman graph formalism from quantum field theory, along with concepts from graph theory. This method provides a graphical representation of both the solution and truncated moments, offering a more intuitive and systematic approach for studying the SPDE and extracting information about the moments of the solutions and the noise ξ. For more details, see, e.g., [10, 12].

Use graph theory concepts such as network graphs, adjacency matrices, or other graph representations to visualize the relationships between the solution components and the moments. We can also consider using tools like network analysis to identify important nodes or substructures within the graph.

The Feynman graph formalism represents the solution $u(t, x)$ of the SPDE (1) and its truncated moments $< u^n(t, x) >^T$ as a sum over specific Feynman graphs, which are graphical representations of the terms in the power series expansion of the solution; see, e.g., [11, 12].

By obtaining graphical representations of both the solution and its truncated moments, we can gain deeper insights into the behavior of the various terms in the generalized MBE, as described in Eq (1.1). Additionally, we can explore several applications of the equation across different fields. For example, if the equation describes a physical system, we can discuss how the graphical representations help in understanding the system's dynamics or predicting its behavior under different conditions. If the equation represents a mathematical model in economics or social sciences, we can discuss how the graphical representations aid in analyzing the model's implications or making predictions. In the context of the current problem, we might compute truncated moments of the solution to understand its behavior in terms of central tendency, variability, skewness, etc. Graphically representing these moments can involve plotting them as functions of some parameter or as distributions themselves. Overall, by incorporating concepts from graph theory and graphical representations, we can gain deeper insights into the solution of the equation and its implications across various domains. This approach also allows for clearer visualization and communication of complex mathematical concepts.

Let us now outline the structure of this paper: In the next section, we introduce key results necessary for this work and present a perturbative solution to the SPDE (1). Section 3 provides a graphical representation of the solution. Section 4 focuses on the truncated moments of the solution and their behaviour for large time $t \to \infty$. Finally, in Section 5, we discuss some applications.

2. Perturbative solution of the SPDE

We begin by presenting essential results from Fourier transform theory, discrete Laplacians, gradients, and Green's functions.

Let $\Xi = \mathbb{R} \times L_\delta = x = (t, \mathbf{x}) \mid t \in \mathbb{R}, \mathbf{x} \in L_\delta$ and $\Pi_\delta^d \cong [0, \frac{2\pi}{\delta}]^d$. Let A be either L_δ or Ξ. The Schwartz space of all rapidly decreasing functions on A, endowed with the Schwartz topology, is denoted by $S(A)$. Its topological dual, the space of tempered distributions, is denoted by $S'(A)$. The dual pairing

between elements of $S(A)$ and $S'(A)$ is denoted by $\langle\cdot,\cdot\rangle$. The action of Fourier transform and discrete Laplacian on a test function u will be given below; however, we refer to [10, 11] for more details.

For $u \in S(\Xi)$, $\int u(x)\,dx = \sum_{x\in L_\delta}\delta^d\int_{\mathbb{R}} u(t,\mathbf{x})dt$, $x = (t,\mathbf{x})$. For $u \in S(L_\delta)$, $\int f(\mathbf{x})d\mathbf{x} = \sum_{x\in L_\delta}\delta^d u(\mathbf{x})$.Let $\mathcal{F} : S(\Xi) \longrightarrow \mathbb{R}\times\Pi_\delta^d$ be the Fourier transform on $S(\Xi)$, i.e.,

$$\mathcal{F}(u)(s,\,\mathbf{q}) = \hat{u}(s,\,\mathbf{q}) = \int e^{its}e^{i\mathbf{q}.\mathbf{x}}u(x)dx\ ,\ u \in S(\Xi). \tag{2.1}$$

The inverse Fourier transform of, $\mathcal{F}$, is given by

$$u(t,\,\mathbf{x}) = \frac{1}{(2\pi)^{d+1}}\int_{\mathbb{R}}\int_{\Pi_\delta^d} e^{-ist}e^{-i\mathbf{q}\cdot\mathbf{x}}\mathcal{F}(u)(s,\,\mathbf{q})ds\,d\mathbf{q}, \tag{2.2}$$

and let $\tilde{\mathcal{F}} : S(L_\delta) \longrightarrow \Pi_\delta^d$ be the Fourier transform on $S(L_\delta)$, i.e.,

$$\tilde{\mathcal{F}}(u)(\mathbf{q}) = \int e^{i\mathbf{q}.\mathbf{x}}u(\mathbf{x})d\mathbf{x}\ ,\ u \in S(L_\delta). \tag{2.3}$$

The inverse Fourier transform of, $\tilde{\mathcal{F}}$ is given by:

$$u(\mathbf{x}) = \frac{1}{(2\pi)^d}\int_{\Pi_\delta^d} e^{-i\mathbf{q}.\mathbf{x}}\tilde{\mathcal{F}}(u)(\mathbf{q})d\mathbf{q}. \tag{2.4}$$

By definition the action, of the Lattice Laplacian Δ on a test function $u \in S(L_\delta)$ is as follows:

$$\Delta u(\mathbf{x}) = \delta^{-2}[-2d\,u(\mathbf{x}) + \sum_{|\mathbf{x}-\mathbf{y}|=\delta} u(\mathbf{y})]. \tag{2.5}$$

Then

$$\tilde{\mathcal{F}}(\Delta f)(\mathbf{p}) = \delta^{-2}\Big[-2d + 2\sum_{j=1}^{d}\cos(\delta\mathbf{p}_j)\Big]\tilde{\mathcal{F}}(u)(\mathbf{q}). \tag{2.6}$$

Where $\mathbf{q}_j = \mathbf{q}\cdot e_j$, and $e_j = (0, ..., 1, 0, ...)$ is the canonical basis of $\mathbb{R}^d$.

We introduce the convolution product " $*$ " as

$$f * g(x) = \int f(x-y)g(y)\,dy,\quad f,\,g \in S(\Xi). \tag{2.7}$$

For $i = 1, \ldots, d$, $|\nabla u(t,\mathbf{x})|^2$ can be written as

$$|\nabla u(t,\mathbf{x})|^2 = \delta^{-2}\sum_{i=1}^{d}\left(u(t,\mathbf{x}+\delta\mathbf{e}_i) - u(t,\mathbf{x})\right)^2, \tag{2.8}$$

and for $p \in \mathbb{N}$

$$|\nabla u(t,\mathbf{x})|^p = \delta^{-p}\sum_{i=1}^{d}\left(u(t,\mathbf{x}\pm\delta\mathbf{e}_i) - u(t,\mathbf{x})\right)^p. \tag{2.9}$$

Therefore, from Eq (2.5), one thus obtain

$$\begin{aligned}\Delta\,|\nabla u(\mathbf{x})|^p &= \delta^{-p}\sum_{i=1}^{d}\Delta\,(u(\mathbf{x}\pm\delta\mathbf{e}_i)-u(\mathbf{x}))^p\\ &= \delta^{-p}\sum_{i=1}^{d}\sum_{k=0}^{p}(-1)^k\binom{p}{k}\Delta\Big(u^k(u\mathbf{x})\,u^{p-k}(\mathbf{x}\pm\delta\,\mathbf{e_i})\Big) \qquad (2.10)\\ &= \delta^{-(p+2)}\sum_{i=1}^{d}\sum_{k=0}^{p}(-1)^k\binom{p}{k}\Big[-2d\,u^k(\mathbf{x})\,u^{p-k}(\mathbf{x}\pm\delta\,\mathbf{e_i})+\sum_{|\mathbf{x}-\mathbf{y}|}u^k(\mathbf{y})\,u^{p-k}(\mathbf{y}\pm\delta\,\mathbf{e_i})\Big].\end{aligned}$$

Therefore

$$\begin{aligned}\tilde{\mathcal{F}}\Big(\Delta\,|\nabla u(\mathbf{x})|^p\Big)(s,\,\mathbf{q}) &= \delta^{-(p+2)}\sum_{i=1}^{d}\sum_{k=0}^{p}(-1)^k\binom{p}{k}\Big[-2d\,\tilde{\mathcal{F}}(u^k(\mathbf{x}))(\mathbf{q})*\tilde{\mathcal{F}}(u^{p-k}(\mathbf{x}+\delta\mathbf{e_i}))(\mathbf{q})\\ &\quad+\sum_{|\mathbf{x}-\mathbf{y}|}\tilde{\mathcal{F}}(u^k(\mathbf{y}))(\mathbf{q})*\tilde{\mathcal{F}}(u^{p-k}(\mathbf{y}\pm\delta\mathbf{e_i}))(\mathbf{q})\Big]\\ &= \delta^{-(p+2)}\sum_{i=1}^{d}\sum_{k=0}^{p}(-1)^k\,C_d\,(i\mathbf{q})^p\binom{p}{k}\Big[\mathcal{F}(u(x))(\mathbf{q})*\mathcal{F}(u(y))(\mathbf{q})\Big],\end{aligned}$$

for $C_d\in\mathbb{R}$, and $|\,\mathbf{x}-\mathbf{y}\,|=\delta$, but

$$\tilde{\mathcal{F}}(u^k(\mathbf{x}))(\mathbf{q})*\tilde{\mathcal{F}}(u^{p-k}(\mathbf{y}))=\int u^k(\mathbf{q}-\mathbf{r})\,u^{p-k}(\mathbf{r})\,d\mathbf{r}. \qquad (2.11)$$

We define now the Green function $G(t,\,\mathbf{x})$ by:

$$\begin{cases}\frac{\partial G(t,\mathbf{x})}{\partial t}=-m\,\nabla^2G(t,\,\mathbf{x})-c\nabla^4G(t,\,\mathbf{x})+\delta(x),\\ G(t,\,\mathbf{x})=0,\quad t<0,\end{cases} \qquad (2.12)$$

where $\delta(x)$ is the Dirac distribution defined by $\delta(x)=\delta(t)\delta(\mathbf{x})=\delta(t)\delta^{-d}\delta_{0,\,\mathbf{x}}$ and $\delta(t)$ is the Dirac distribution on $\mathbb{R}$ and $\delta_{\mathbf{x},\mathbf{y}}=\prod_{l=1}^{d}\delta_{\delta^{-1}x_l,\delta^{-1}y_l}$ with $\delta_{i,j}$ the Kronecker symbol.

Applying to the Fourier transform $\mathcal{F}$, it is obvious that

$$\mathcal{F}(G)(s,\,\mathbf{q})=\frac{1}{-is+\alpha_{m,\,c}(\mathbf{q})}\ , \qquad (2.13)$$

where

$$\alpha_{m,\,c}(\mathbf{q})=2\,\delta^{-2}\,m\Big(d-m\sum_{j=1}^{d}\cos(\delta\mathbf{p_j})\Big)\ +\ 4\,c\,\delta^{-4}\Big(d-\sum_{j=1}^{d}\cos(\delta\mathbf{p_j}+\cos(\delta\mathbf{p_j}+\delta\mathbf{e_j})\Big). \qquad (2.14)$$

Here $\mathbf{e_j}=(0,...,1,0,...)$ is the canonical basis of $\mathbb{R}^d$ and $\mathbf{p_j}=\mathbf{p}\,.\,\mathbf{e_j}$.

We introduce another Green function $\tilde{G}_t$ as follows:

$$G(t,\,\mathbf{x})=\theta(t)\tilde{G}_t(\,\mathbf{x}), \qquad (2.15)$$

where $\theta(t)=1$ if $t>0$ and $\theta(t)=0$ else.

Lemma 2.1. $\forall\ N \in \mathbb{N},\ \exists\ \beta_N$ *such that:*

$$| G(s,\ \mathbf{p}) | \leq\ \beta_N\ \frac{e^{-\frac{t}{2}}}{(1+ | \mathbf{p} |^2)^N},\quad (s,\ \mathbf{p})\ \in\ ]0,\ \infty[\times L_\delta. \tag{2.16}$$

Proof. We have

$$\begin{aligned} G(s,\mathbf{p}) &= \frac{1}{(2\pi)^d}\int_{[0,\frac{2\pi}{\delta}]^d} e^{i\mathbf{q}.\mathbf{p}} e^{-t\alpha_{m,c}(\mathbf{q})} d\mathbf{q} \\ &= \frac{e^{\frac{-t}{2}}}{(2\pi)^d(1+|\mathbf{p}|^2)^N}\int_{[0,\frac{2\pi}{\delta}]^d}\left[(1-\Delta)^N e^{i\mathbf{q}.\mathbf{p}}\right] e^{-t\alpha_{m,c}(\mathbf{q})} d\mathbf{q} \\ &= \frac{e^{\frac{-t}{2}}}{(2\pi)^d(1+|\mathbf{p}|^2)^N}\int_{[0,\frac{2\pi}{\delta}]^d} e^{i\mathbf{q}.\mathbf{p}}\left[(1-\Delta)^N e^{-t\alpha_{m,c}(\mathbf{q})}\right] d\mathbf{q}, \end{aligned} \tag{2.17}$$

thus the integrand is a product of a bounded function with norm 1 and a polynomial function $P(t,\mathbf{q}) = (1-\Delta)^N e^{-t\,\alpha_{m,c}(\mathbf{q})}$, hence

$$| G(s,\ \mathbf{p}) | \leq\ \beta_N\ \frac{e^{-\frac{t}{2}}}{(1+ | \mathbf{p} |^2)^N},\quad (s,\ \mathbf{p})\ \in\ ]0,\ \infty[\times L_\delta, \tag{2.18}$$

where $\beta_N = \frac{1}{(2\pi)^d} \sup\limits_{\substack{t>0 \\ \mathbf{q}\in\left[0,\frac{2\pi}{\delta}\right]^d}} | (1-\Delta)^N e^{-t\,\alpha_{m,c}(\mathbf{q})} |$.

Lemma 2.2. *Let $\mathcal{S}$ be the set of all measurable functions $f : \Lambda \to \mathbb{R}$ such that for any $k \in \mathbb{N}, \exists N \in \mathbb{N}$ and*

$$\int_\Xi \frac{|f(x)|^k}{(1+|x|^2)^N} dx < \infty.$$

Then, $\mathcal{S}$ is an algebra under multiplication. In addition, if $h \in \mathcal{S}$, then $G * h \in \mathcal{S}$.

Proof. For the proof we refer to [10]. □

For $i = 1, ..., d$, we denote by $\mathbf{Z}$ be the random variable given by the distribution

$$P\left(\mathbf{Z} = \pm\delta\mathbf{e}_i\right) = \frac{1}{d}, \tag{2.19}$$

here $\mathbf{e_i} = (0, ..., 1, 0, ...)$ is the canonical basis of $\mathbb{R}^d$.

Proposition 2.1. *Let $u(t,\ \mathbf{x}) = \sum_{j=0}^{\infty}(-\beta)^j u_j(t,\ \mathbf{p})$ be an expansion of u in the sense of formal power series in the parameter β and assume that $G * \eta \in \mathcal{S}$ a.s. The perturbative solution of the stochastic partial differential equation (1.1) is given by*

$$\begin{cases} u_0(t,\ \mathbf{x}) = G * \xi(t,\ \mathbf{x}) + \tilde{G}_t \star \phi(\mathbf{x}), \\ u_j(t,\ \mathbf{x}) = G * \displaystyle\sum_{L_p^j(i_0,\,i_1,\ldots)} K_{d,\delta}\,\frac{k!(p-k)!}{i_0!i_1!\ldots}\prod_{m\geq 0} u_m^{i_m}(t,\mathbf{x})\,u_m^{i_m-k}(t,\mathbf{x}+\ \mathbf{Z}),\quad j \geq 1, \end{cases} \tag{2.20}$$

with $u_j \in \mathcal{S}$ a.s, here $L_p^j(i_0,\ i_1,\ ...) = \{i_0,\ i_1,\ ...\geq\ 0\ \mid\ i_0+i_1+...=p\,;k=0,1,...,p\,;\ \sum\limits_{m\,\geq\,0} m\,i_m\ =\ j-1\}$ and $K_{d,\delta} \in \mathbb{R}$.

Proof. We have the integrated form of the SPDE (1):

$$u(t,\mathbf{x}) = \beta\, G * \nabla^2 \mid \nabla u(t,\mathbf{x}) \mid^p + G * \xi(t,\ \mathbf{x}) + \tilde{G}_t \star \phi(\mathbf{x}). \tag{2.21}$$

By setting $u(t,\mathbf{x}) = \sum_{j=0}^{\infty} \beta^j\, u_j(t,\mathbf{x})$ and for $\beta = 0$, we get for $j = 0$:

$$u_0(t,\mathbf{x}) = G * \xi(t,\ \mathbf{x}) + \tilde{G}_t \star \phi(\mathbf{x}). \tag{2.22}$$

On the other hand for $j \geq 1$ and from Eq (2.10), we have

$$\begin{aligned}
\sum_{j=0}^{\infty} \beta^j\, u_j(t,\mathbf{x}) &= \beta\, G * \nabla^2 \mid \nabla u(t,\mathbf{x}) \mid^p + G * \xi(t,\ \mathbf{x}) + \tilde{G}_t \star \phi(\mathbf{x}) \\
&= \delta^{-(p+2)} \sum_{i=1}^{d} \sum_{k=0}^{p} (-1)^k \binom{p}{k} \beta \Big[-2d\, (\sum_{j=0}^{\infty} \beta^j u_j(t,\mathbf{x}))^k\, (\sum_{j=0}^{\infty} \beta^j u_j(t,\mathbf{x} \pm \delta\, \mathbf{e_i}))^{p-k} \\
&\quad + \sum_{|\mathbf{x}-\mathbf{y}|} (\sum_{j=0}^{\infty} \beta^j u_j(t,\mathbf{y}))^k\, (\sum_{j=0}^{\infty} \beta^j u_j(t,\mathbf{y} \pm \delta\, \mathbf{e_i}))^{p-k} \Big] + G * \xi(t,\ \mathbf{x}) + \tilde{G}_t \star \phi(\mathbf{x}) \\
&= G * \sum_{\substack{i_0, i_1, \ldots \geq 0 \\ i_0 + i_1 + \ldots = p \\ k = 0,1,\ldots,p}} K_{d,\delta}\, \frac{k!(p-k)!}{i_0! i_1! \ldots}\, \prod_{m \geq 0} \beta^{m i_m}\, u_m^{i_m}(t,\mathbf{x})\, u_m^{i_m - k}(t,\mathbf{x} \pm \delta\, \mathbf{e_i}),
\end{aligned} \tag{2.23}$$

for some constant $K_{d,\delta}$. Hence by identification

$$u_j(t,\ \mathbf{x}) = G * \sum_{L_p^j(i_0,\, i_1, \ldots)} K_{d,\delta}\, \frac{k!(p-k)!}{i_0! i_1! \ldots}\, \prod_{m \geq 0} u_m^{i_m}(t,\mathbf{x})\, u_m^{i_m - k}(t,\mathbf{x} + \mathbf{Z}), \quad j \geq 1, \tag{2.24}$$

where $L_p^j(i_0,\ i_1,\ \ldots) = \{i_0,\ i_1,\ \ldots \geq 0 \ \mid \ i_0 + i_1 + \ldots = p\,; k = 0, 1, \ldots, p\,;\ \sum_{m \geq 0} m\, i_m = j - 1\}$. □

3. Graph expansion of the perturbative solution

The solution presented in Proposition 2.1 through Eq (2.20) is technically complex and does not provide clear insights into the behavior of the solution or the truncated moments. Introducing concepts from graph theory to represent the solution and truncated moments offers an effective way to visualize and analyze complex systems, such as molecular beam epitaxy (MBE) problems modeled by Eq (1.1). This approach allows for the evaluation of various aspects of MBE, including growth dynamics, surface smoothness, and pattern formation during the epitaxial process. Graph theory provides a robust framework for understanding the relationships and structures within the data. We will use graph theory to represent the solution of the equation, where each node in the graph represents a variable or component of the solution, and the edges depict the interactions or relationships between these components. This graphical representation can facilitate the visualization of the solution's structure and the identification of key components.

Truncated moments of the solution capture statistical properties of a distribution, often used in probability theory and statistics.

Let us remind you that a graph G consists of a nonempty set $V(G)$ of vertices together with a finite set $E(G)$ of edges such that each edge joins two distinct vertices in $V(G)$ and any two distinct vertices in $V(G)$ are joined by a finite number of edges. The order of the graph G consists of the number of vertices in G.

The graph G is said to be connected if each two vertices in G can be joined by a path. For more details about the graph theory concepts we refer to, for example [14, 15].

Definition 3.1. *A tree T is a connected graph without cycles.*

In the following we denote by $\mathcal{T}(i)$ the set of all rooted trees T with root $x = (t, \mathbf{x})$ and four types of leaves, which has i inner vertices with $p + 1$ legs. For the reader's convenience, the table and examples below summarize the graphical representations of the inner vertices, edges, and leaves of the tree T as well as examples of trees of type 0 and 1 corresponding to $T \in \mathcal{T}(0)$ and $T \in \mathcal{T}(1)$, respectively:

G	Leaf of type 1 $\xi(t, \mathbf{x})$	leaf of type 2 $\phi(\mathbf{x})$	Leaf of type 3 $\xi(t, \mathbf{x} + \mathbf{Z})$	leaf of type 4 $\phi(\mathbf{x} + \mathbf{Z})$	Root of a tree T	Inner vertex
———	⊙	∅	⊙	⊗	╳	●

The representations of a tree of order 0 and 1 are given below:

Tree of order 0

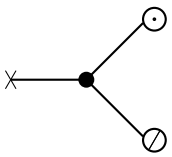

Tree of order 1

Definition 3.2. *For $T \in \mathcal{T}(i)$, $i \geq 0$, we define the analytic value $\mathcal{V}(T, x, \xi)$ as follows:*

Vertices and leaves values assignments

- *Assign $x \in \Xi$ to the root of the tree T.*
- *Assign values $x_1, \ldots, x_n \in \Xi$ to the inner vertices.*
- *Assign $y_1, \ldots, y_l \in \Xi$ to the leaves of type 1 and $\mathbf{z_1}, \ldots, \mathbf{z_k} \in L_\delta$ to the leaves of type 2, where $l, k \in \mathbb{N}$.*
- *Assign $t_1, \ldots, t_q \in \Xi$ to the leaves of type 3 and $\mathbf{r_1}, \ldots, \mathbf{r_m} \in L_\delta$ to the leaves of type 4, where $q, m \in \mathbb{N}$.*

Edge value assignments

- *For every edge e with two endpoints, $e = \{v, w\}$, assign a value $G(e) = G(v - w)$ if e is connected to a leaf of type 1 or 3, or $\hat{G}_t(e)$ if it is connected to a leaf of type 2 or 4. Here, G and $\hat{G}_t$ are the Green functions defined in (2.12) and (2.15).*

Multiplications rules

- *If a vertex v_0 is connected to two leaves, one of type 1 or 2 and the other of type 3 or 4, multiply the result by (-2).*
- *For the j-th leaf, multiply its corresponding value by $\xi(y_j)$, $\phi(\mathbf{z}_j)$, $\xi(t, \mathbf{u_j} + \mathbf{Z})$ or $\phi(\mathbf{v_j} + \mathbf{Z})$ if this leaf is of type 1, 2, 3, or 4, respectively.*

- *Multiply the result by a constant $K_{d,\delta}$.*

Integration

- *Integrate with respect to the Lebesgue measure $dx_1 \cdots dx_n dy_1 \cdots dy_l dz_1 \cdots dz_k$.*

Theorem 3.1. *Let $T \in \mathcal{T}(j)$, $j \geq 0$, be a rooted tree with j inner vertices. Then, the solution u_j of the stochastic partial differential equation* (1) *in the sense of formal power series is given by*

$$u_j(t, \mathbf{x}) = \sum_{T \in \mathcal{T}(i)} \mathcal{V}(T, x, \xi), \quad j \geq 0. \tag{3.1}$$

Proof. We prove the assertion by induction. For $j = 0$, we have $u_0(x, \eta) = G * \xi(x) + \tilde{G}_t * \phi(\mathbf{x})$, which is just the sum of the evaluation of the two trees in $\mathcal{T}(0)$.

Suppose that (3.1) is true for all $i < j$. By proposition (2.20) we have

$$u_j(t, \mathbf{x}) = G * \sum_{L_p^j(i_0, i_1, \ldots)} K_{d,\delta} \frac{k!(p-k)!}{i_0! i_1! \ldots} \prod_{m \geq 0} u_m^{i_m}(t, \mathbf{x})\, u_m^{i_m - k}(t, \mathbf{x} + \mathbf{Z}), \quad j \geq 1. \tag{3.2}$$

Then using the induction hypothesis and definition (3.2) we obtain

$$\begin{aligned} u_j(t, \mathbf{x}) &= G * \sum_{L_p^j(i_0, i_1, \ldots)} K_{d,\delta} \frac{k!(p-k)!}{i_0! i_1! \ldots} \prod_{m \geq 0} u_m^{i_m}(t, \mathbf{x})\, u_m^{i_m - k}(t, \mathbf{x} + \mathbf{Z}) \\ &= \sum_{L_p^j(i_0, i_1, \ldots)} K_{d,\delta} \frac{k!(p-k)!}{i_0! i_1! \ldots} \Big(G * \prod_{m \geq 0} u_m^{i_m}(t, \mathbf{x})\, u_m^{i_m - k}(t, \mathbf{x} + \mathbf{Z}) \Big) \\ &= \sum_{L_p^j(i_0, i_1, \ldots)} K_{d,\delta} \frac{k!(p-k)!}{i_0! i_1! \ldots} \sum_{T_1, T_2, \ldots, T_n \in \mathcal{T}(i)} \prod_{i \geq 0} \mathcal{V}(T_i, x, \xi) \\ &= \sum_{T \in \mathcal{T}(j)} \mathcal{V}(T, x, \xi). \end{aligned} \tag{3.3}$$

□

The following examples illustrates the applications of definition (3.2) and theorem (3.1). We then present graphical representations of the solutions u_0 and u_1, respectively:

$$\begin{aligned} u_0(t, \mathbf{x}) &= G \star \xi(t, \mathbf{x}) + \hat{G}_t * \phi(\mathbf{x}) \\ &= \text{✗——⊙} + \quad \text{✗——⊘} \end{aligned} \tag{3.4}$$

and

$$u_1(t, \mathbf{x}) = G \star \Big[u_0^2(t, \mathbf{x}) \Big(u_0^2(t, \mathbf{x} + \mathbf{Z}) + u_0(t, \mathbf{x} + \mathbf{Z}) + 2 \Big) \Big] \tag{3.5}$$

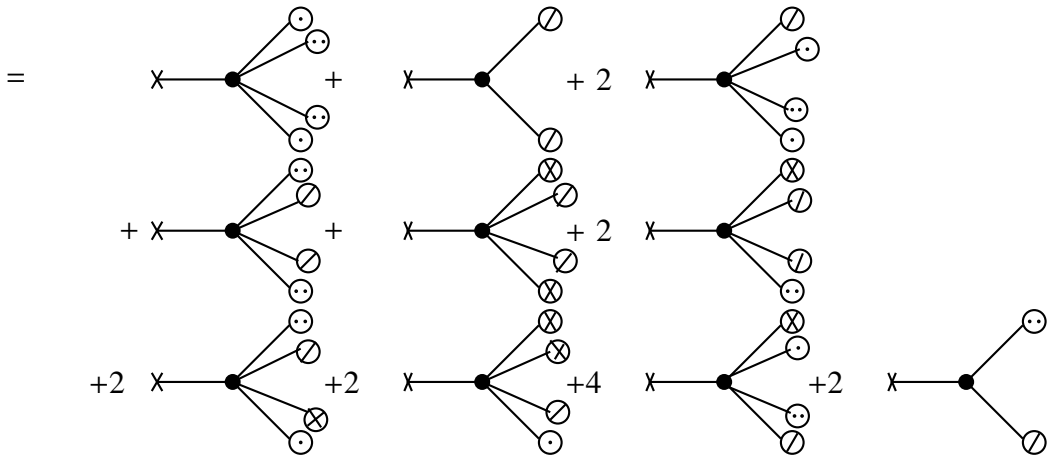

4. Truncated moments of the solutions

In this section, we will compute the moments of the solutions discussed in the previous section. Additionally, we will introduce new graphs and provide graphical representations of the correlation function. These graphs comprise n rooted trees $T_1 \in \mathcal{T}(i_1), ..., T_n \in \mathcal{T}(i_n)$ as subgraphs with 4 types of leaves and m inner vertices such that any leave of type 1 or 3 is connected to a new vertex called "inner empty vertex" and represented by ○ We denote such a graph by $\mathcal{A}$ and the set of all graphs of $m-$th order and n roots by $\mathcal{P}(m, n)$. Towards the conclusion of this section, we will delve into the behavior of the solutions as time t approaches infinity, reaching equilibrium.

By definition, inner vertices are distinguishable and have non-distinguishable legs whereas empty vertices are non-distinguishable and have non-distinguishable legs.

Proposition 4.1. *For $j_1, ..., j_n \in \mathbb{N}$, let $T_1 \in \mathcal{T}(j_1), ..., T_n \in \mathcal{T}(j_n)$ be n rooted trees with roots $x_1, ..., x_n \in \Xi$, then the following result holds in the sense of formal power series*

$$\left\langle \prod_{i=1}^{n} u(x_i, \eta) \right\rangle = \sum_{m=0}^{\infty} \beta^m \sum_{\substack{j_1, ..., j_n \geq 0 \\ j_1 + ... j_n = m \\ T_1 \in \mathcal{T}(j_1), ..., T_n \in \mathcal{T}(j_n)}} \left\langle \mathcal{V}_1(T_1, x_1, \eta) \cdots \mathcal{V}_n(T_n, x_n, \eta) \right\rangle. \tag{4.1}$$

Proof.

$$\begin{aligned} \left\langle \prod_{i=1}^{n} u(x_i, \eta) \right\rangle &= \left\langle \sum_{j=0}^{\infty} \beta^j u_j(x_1, \eta) \cdots \sum_{j=0}^{\infty} \beta^j u_j(x_n, \eta) \right\rangle \\ &= \sum_{m=0}^{\infty} \lambda^m \sum_{\substack{j_1, ..., j_n \geq 0 \\ j_1 + ... + j_n = m}} \left\langle u_{j_1}(x_1, \eta) \cdots u_{j_n}(x_n, \eta) \right\rangle \\ &= \sum_{m=0}^{\infty} \lambda^m \sum_{\substack{j_1, ..., j_n \geq 0 \\ j_1 + ... + j_n = m \\ T_1 \in \mathcal{V}(j_1), ..., T_n \in \mathcal{V}(j_n)}} \langle \mathcal{V}_1(T_1, x_1, \eta) \cdots \mathcal{V}_n(T_n, x_n, \eta) \rangle . \end{aligned} \tag{4.2}$$

The last equality is an immediate consequence of Theorem 3.1. □

Definition 4.1. Let $x_1, ..., x_k \in \Xi$, I a partition of the set $\{1, ..., n\}$, $I \in \mathcal{D}(\{1, ..., n\})$, $E = \{E_1, ..., E_k\}$ the truncated moments functions $\langle \xi(x_1) \cdots \xi(x_n) \rangle^T$ are recursively defined by:

$$\langle \prod_{i=1}^{n} \xi(x_i) \rangle = \sum_{\substack{I \in \mathcal{D}(\{1,...,n\}) \\ E=\{E_1,...,E_k\}}} \prod_{l=1}^{k} \langle E_l \rangle^T, \tag{4.3}$$

where $\langle E_l \rangle^T = \langle \prod_{j \in E_l} \xi(x_j) \rangle^T$.

We will now define a new graph $\mathcal{A}(m, n)$ with 4 types of leaves and m inner vertices, the leaves of types 1 and 3 will be connected by empty vertices ○ . In the following we provide a detailed methodology to construct and assign values within the graph $\mathcal{A}(m, n)$ combining various mathematical elements like Green functions, specific multiplication rules, and integrations. The final step involves integrating with respect to the given Lebesgue measures to obtain the desired result.

The set of such graphs is denoted by $\mathbb{P}(m, n)$.

To summarize the construction and assignment of values in the new graph $\mathcal{A}(m, n)$, here is a step-by-step breakdown:

Definition 4.2. *Let $T_1 \in \mathcal{T}(i_1), ..., T_n \in \mathcal{T}(i_n)$ be n rooted trees, we define a graph $\mathcal{A}(m, n)$ with m inner vertices and 4 types of leaves, such that leaves of types 1 and 3 are connected by empty vertices, as follows:*

Value assignments

- *Assign values $x_1, \ldots, x_n \in \Xi$ to the roots of the trees $T_1, \ldots, T_n$.*
- *Assign values $m_1, \ldots, m_p \in \Xi$ to the inner vertices.*
- *Assign values $y_1, \ldots, y_l \in \Xi$ to the leaves of type 1.*
- *Assign values $z_1, \ldots, z_k \in L_\delta$ to the leaves of type 2.*
- *Assign values $u_1, \ldots, u_q \in \Xi$ to the leaves of type 3.*
- *Assign values $r_1, \ldots, r_p \in L_\delta$ to the leaves of type 4.*

Special multiplication rule

- *If a vertex v is connected to two leaves, one of type 1 or 2 and the other of type 3 or 4, multiply the result by (-2).*

Edge value assignments

- *Assign a value $G(e)$ to each edge e if it is connected to a leaf of type 1 or 3.*
- *Assign a value $\hat{G}_t(e)$ if the edge e is connected to a leaf of type 2 or 4.*
- *Here, G and $\hat{G}_t$ are the Green functions defined by Eqs (2.12) and (2.15).*

Empty vertex multiplication

- *For each empty vertex with i legs connected to the leaves 1 and 3 with arguments $r_1, \ldots, r_i$, multiply with*

$$\langle \xi(r_1) \cdots \xi(r_i) \rangle^T .$$

Leaf multiplications

- *For the leaves of type 2, multiply with* $\phi(y_j)$.
- *For the leaves of type 4, multiply with* $\phi(z_s + \mathbf{Z})$.
- *Here,* $j = 1, \ldots, k$ *and* $s = 1, \ldots, r$.

Constant multiplication

- *Multiply the entire expression by the constant* $K_{d,\delta}$.

Integration

- *Integrate the final expression with respect to the Lebesgue measure* $dy_1 \cdots dy_l\, dz_1 \cdots dz_k$.

As an example of the above graph, we provide a representation of a graph $\mathcal{A}$ obtained as a combination of two trees, $T_1, T_2 \in \mathcal{T}(1)$, with 4 and 2 leaves, respectively; see Figure 1.

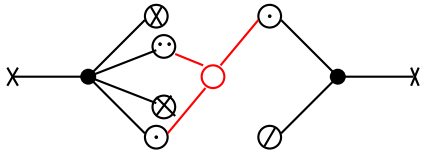

Figure 1. Graph $\mathcal{A}(2,2)$.

Its analytic value is

$$\begin{aligned}\mathcal{L}(\mathcal{G}) \;=\; & \int G(x_1 - x)G(x_2 - x_1)G(x_3 - x_1)G(x_4 - x_1)G(x_5 - x_1)G(y - y_1)G(y_2 - y_1)G(y_3 - y_1) \\ & \times \langle \xi(x_3)\xi(\mathbf{x_5} + \mathbf{Z})\xi(y_2)\rangle^T \, \phi(\mathbf{y_3})\, \phi(\mathbf{x_3} + \mathbf{Z})\phi(\mathbf{x_4} + \mathbf{Z})\, dx_1 \cdots dx_5 dy_1 \cdots dy_3, \\ & \qquad x_1, \cdots x_5,\ y_1, \cdot y_3 \in \Xi,\ \ \mathbf{y_3}, \mathbf{x_3}\, \mathbf{x_4}\, \mathbf{x_5} \ \in \ L_\delta. \end{aligned} \tag{4.4}$$

Theorem 4.1. *Given that* $T_1, \ldots, T_n$, *n rooted trees with roots* $x_1, \ldots, x_n \in \Xi$, *respectively. Then, the moment of the solution is given by a sum over all graphs* $\mathcal{A} \in \mathbb{P}(m, n)$ *of m-th order, i.e.,*

$$\left\langle \prod_{i=1}^{n} u(x_i, \xi) \right\rangle = \sum_{m=0}^{\infty} (-\beta)^m \sum_{\mathcal{A} \in \mathbb{P}(m,n)} \mathcal{L}(\mathcal{G})(x_1, \ldots, x_n). \tag{4.5}$$

Proof. The proof is immediate from Proposition 4.1 and Definition 4.2. □

5. Correlation function and equilibrium: A case of Lévy noise

In this section, we begin with some standard results on stochastic processes, focusing specifically on key topics related to Lévy processes that are essential for achieving our results. For further details, we refer the reader to [16].

A Lévy process $\{u_t, t \geq 0\}$ defined on $\mathbb{R}^d$ is a stochastic process with independent and stationary increments such that $u_0 = 0$, a.s, and continuous in probability, i.e., for any $\epsilon > 0$ and $t \geq 0$ it holds that $\lim_{h \longrightarrow 0} P(|u_{t+h} - u_t| > \epsilon) = 0$.

Let $\xi_t = \xi(t), t \geq 0$, be a Lévy process on $\mathbb{R}^d$; following [16], it can be represented by

$$\xi(t) = m\,t + k\,B_t + \int_0^t \int_{|\zeta|<1} \zeta\,\tilde{N}(ds, d\zeta) + \int_0^t \int_{|\zeta|\geq 1} \zeta\,N(ds, d\zeta), \tag{5.1}$$

where $\tilde{N}$ is a compensated jump measure, $B_t = B(t),\ t \geq 0$ is a standard Brownian motion on $\mathbb{R}^d$, m and k are constants.

Let Ψ be the Lévy characteristic associated to ξ_t, following [16]; Ψ is given by

$$\Psi(a) = i\langle l, a\rangle - \langle a, b\,a\rangle + \int_{\mathbb{R}^d\setminus\{0\}} (e^{i\langle x,a\rangle} - 1)\,\nu(dx),\ a \in \mathbb{R}^d. \tag{5.2}$$

Here $l,\ b \in \mathbb{R}^d$ and ν is a positive Lévy measure satisfying:

$$\int_{|x|\leq 1} |x|\,\nu(dx) < \infty, \quad \int_{|x|\geq 1} |x|^2\,\nu(dx) < \infty,$$

then, the transition probability density of the solution $u_t,\ t \geq 0$, can be characterized by the Fourier transform:

$$\mathcal{F}(e^{-t\,\Psi(\zeta)})(x) = (2\pi)^{-d} \int_{\mathbb{R}^d} e^{-x\cdot\zeta}\,e^{-t\,\Psi(\zeta)}\,d\zeta.$$

Theorem 5.1. *Let ξ be a Lévy space-time noise and $x_1, \ldots, x_n \in \Lambda$. Then the following result holds:*

$$\Big\langle \prod_{i=1}^{n} \xi(x_i) \Big\rangle^T = C_n \int \delta(x - x_1) \cdots \delta(x - x_1)dx, \tag{5.3}$$

where

$$C_n = (-i)^n \frac{d^n\Psi(t)}{dt^n}\Big|_{t=0} = \delta_{n,1}a - \delta_{n,2}\sigma^2 + \int_{\mathbb{R}-\{0\}} s^n dr(s) \tag{5.4}$$

and $\delta_{n,m}$ is the Kronecker symbol.

Proof. For the proof we refer to [17]. □

Theorem 5.1 simplifies the empty vertex multiplication described in Definition 4.2, as it replaces the expression with $C_n \int \delta(x-x_1)\cdots\delta(x-x_1)dx$, where C_n are the $n-th$ moments given by Eqs (5.2)–(5.4). This leads to a simplified value $\hat{\mathcal{L}}$ for the graph $\mathcal{G} \in \mathbb{G}(m, n)$.

Theorem 5.2. *Consider n rooted trees $T_1, \ldots, T_n$, with corresponding roots $x_1, \ldots, x_n$, respectively. Then the moments of the solution are given by*

$$\Big\langle \prod_{i=1}^{n} u(x_i, \eta) \Big\rangle = \sum_{m=0}^{\infty} (-\lambda)^m \sum_{\mathcal{G}\in\mathbb{P}(m,n)} \hat{\mathcal{L}}(\mathcal{G})(x_1, \ldots, x_n). \tag{5.5}$$

Proof. The proof is a consequence of Definition (4.2), Theorems (4.1) and (5.1) . □

For clarity, the graphical representation in Figure 1 is simplified to the following graph in Figure 2, based on the application of Theorem 5.1.

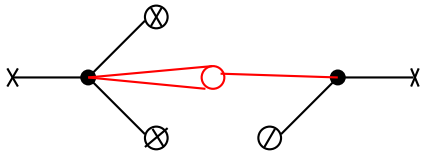

Figure 2. Simplified graph $\mathcal{A}(2,2)$.

The analytic value becomes then

$$\begin{aligned}\mathcal{L}(\mathcal{G}) &= C_3 \int G(x_1 - x)G(x_2 - x_1)G(x_4 - x_1)G(y - y_1)G(y_3 - y_1)\phi(\mathbf{y_3})\,\phi(\mathbf{x_3} + \mathbf{Z}) \\ &\quad \times \phi(\mathbf{x_4} + \mathbf{Z})\;\; dx_1 dx_2 dx_4\, dy_1 dy_3, \quad x_1, x_2, x_4,\; y_1, y_3 \in \Xi,\;\; \mathbf{y_3},\; \mathbf{x_3}, \mathbf{x_4} \;\in\; L_\delta,\end{aligned}$$

here $C_3 = \int_{\mathbb{R}-\{0\}} s^3 dr(s)$ are the coefficients given by Eq (5.4).

Definition 5.1.

Graph construction

We define new collections of graphs $\hat{\mathbb{P}}_c(m,n)$ in $\mathbb{P}(m,n)$ that do not possess leaves of type 2 or 4.

Analytic values

The analytic value of a given graph $\hat{\mathcal{G}} \in \hat{\mathbb{P}}_c(m,n)$ is obtained as follows:

(1) Assign the values $x_1, \ldots, x_n \in \Xi$ to the roots of the trees $T_1, \ldots, T_n$.
(2) Assign the values $m_1, \ldots, m_p \in \Xi$ to the inner vertices.
(3) Assign $y_1, \ldots, y_l \in \Xi$ to the leaves of type 1, where $l \in \mathbb{N}$.
(4) i)- Assign $u_1, \ldots, u_q \in \Xi$ to the leaves of type 3 , where $q \in \mathbb{N}$.
ii)- If a vertex v is connected to two leaves, one of type 1 and the other of type 3, multiply the result by (-2).

Edge and constant multiplications

(1) For every edge e, assign a value $G(e)$ to this edge if it is connected to a leaf of type 1 or 3. Here, G is the Green function defined in (2.12) and (2.13).
(2) For each empty vertex with i legs connected to the leaves 1 and 3 with arguments $r_1, \ldots, r_i$, multiply with $\langle \xi(r_1) \cdots \xi(r_i) \rangle^T$.
(3) Multiply by the constant $K_{d,\delta}$.

Integration

(1) Integrate with respect to the Lebesgue measure $dy_1 \cdots dy_l dz_1 \cdots dz_k$.

Lemma 5.1. *Let $\hat{\mathcal{G}} \in \hat{\mathbb{P}}_c(m,n)$ and let $\Gamma(\hat{\mathcal{G}}) = \prod_{e \in E(\hat{\mathcal{G}})} G(e)$, then there exists $L = L(m,n)$ such that*

$$| \Gamma(\hat{\mathcal{G}}) | \leq \frac{L}{(1 + \max_{u,v \in L_1(\hat{\mathcal{G}})} | u - v |^2)(1 + \max_{w,r \in L_3(\hat{\mathcal{G}})} | w - r |^2)}. \tag{5.6}$$

Proof. Let $u, v \in L_1(\hat{\mathcal{G}})$ and $w, r \in L_3(\hat{\mathcal{G}})$; since $\hat{\mathcal{G}}$ is connected, then there exist paths P_1 from u to v and P_2 from w to r. Therefore

$$| \Gamma(\hat{\mathcal{G}}) | \;\; = \prod_{e_1 \in (P_1 \cup P_2)} G(e) \times \prod_{e_3 \in E(\hat{\mathcal{G}}) \setminus (P_1 \cup P_2)} G(e_3)$$

$$= \prod_{e_1=\{u,v\}\in L_1(\hat{\mathcal{G}})} G(u-v) \times \prod_{e_3=\{w,r\}\in L_3(\hat{\mathcal{G}})} G(w-r), \tag{5.7}$$

now the result is immediate using lemma (2.1). □

Theorem 5.3. *Let $\hat{\mathcal{G}} \in \hat{\mathbb{P}}_c(m,n)$, then the perturbation series for the truncated moments converges in the sense of formal power series as t goes to infinity to*

$$\langle \hat{u}(\mathbf{x_1}) \cdots \hat{u}(\mathbf{x_n}) \rangle^T = \lim_{t \longrightarrow \infty} \langle u(x_1) \cdots u(x_n) \rangle^T, \tag{5.8}$$

where

$$\langle \hat{u}(\mathbf{x_1}) \cdots \hat{u}(\mathbf{x_n}) \rangle^T = \sum_{m=0}^{\infty} \beta^m \sum_{\hat{\mathcal{G}} \in \hat{\mathbb{P}}_c(m,n)} \hat{\mathcal{L}}_c(\hat{\mathcal{G}})(\mathbf{x_1}, ..., \mathbf{x_n}). \tag{5.9}$$

Proof. We need to show that $\lim_{t\longrightarrow\infty} \hat{\mathcal{L}}(\hat{\mathcal{G}})\Big((t,x_1),...,(t,x_n)\Big) = 0$, for every $\hat{\mathcal{G}} \in \hat{\mathbb{P}}_c(m,n)$ without leaf of type 2 or 4, but this is valid since leaves of type 2 and 4 do not contribute in this case, and the analytic value of the corresponding graphs is zero. therefore $\lim_{t\longrightarrow\infty} \hat{\mathcal{L}}(\hat{\mathcal{G}})\Big((t,x_1),...,(t,x_n)\Big) = \hat{\mathcal{L}}_c(\hat{\mathcal{G}})(\mathbf{x_1}, ..., \mathbf{x_n})$. Hence using lemma (5.1) the integral over $\Gamma(\hat{\mathcal{G}})$ is 0 as $t \longrightarrow \infty$. □

6. A remark on some applications

Stochastic nonlinear beam epitaxy (SNBE) equations are used in the field of materials science and nanotechnology, particularly in the growth of thin films and nanostructures. Here are some applications of SNBE equations which are inspired by well-known models in surface science and thin-film growth, such as the Kardar-Parisi-Zhang (KPZ) equation, see, e.g., [18]:

Thin film growth: SNBE equations are used to model the growth of thin films with atomic-scale precision. In molecular beam epitaxy (MBE), the height h describing the local position of the moving surface obeys a conservation law given by:

$$\frac{\partial h(x,t)}{\partial t} = -\nabla \cdot J(\nabla h(x,t)) + \eta(x,t), \tag{6.1}$$

where $h(x,t)$ is the height function, $\eta(x,t)$ represents noise or stochastic fluctuations, and $J(\nabla h(x,t))$ is the flux or current density associated with the flow of material.

Clearly-Eq (6.1) is a particular case of the SPDE (1) studied in this paper; the noise η given in Eq (6.1) is in general of Gaussian type, whereas in our current study we considered a Lévey type noise; hence our results can be useful by incorporating stochastic effects and nonlinearity. These equations provide a more realistic description of the growth process, accounting for factors such as surface diffusion, deposition rates, and surface roughness evolution.

Nanostructure fabrication: In addition to thin films, SNBE equations can be applied to the fabrication of nanostructures such as quantum dots, nanowires, and nanorods. These equations help researchers understand how stochastic fluctuations and nonlinear interactions affect the morphology, size distribution, and arrangement of nanostructures during growth.

The stochastic nonlinear beam epitaxy (SNBE) equations used to model the fabrication of nanostructures such as quantum dots, nanowires, and nanorods can vary depending on specific

assumptions and system characteristics. However, a general set of equations might include terms representing growth, diffusion, surface kinetics, and stochastic effects. Here's a simplified representation:

If $h(x, t)$ represents the height of the surface at position x and time t, the general form of SNBE equations for nanostructure fabrication can be written as:

$$\frac{\partial h(x,t)}{\partial t} = -\nabla \cdot J(\nabla h(x,t)) + \eta(x,t). \tag{6.2}$$

This equation describes the evolution of the surface height $h(x, t)$ over time t. Here $\frac{\partial h(x,t)}{\partial t}$ represents the rate of change of the surface height with time, $-\nabla \cdot J(\nabla h(x, t))$ is the flux or current density associated with the flow of material, which is influenced by the gradient of the surface height and $\eta(x, t)$ is the stochastic noise or fluctuations, representing the random nature of the growth process.

The specific form and complexity of the SNBE equations will depend on the level of detail and accuracy required for the particular application or research study. These equations are often solved numerically. However, by using our graph formalism approach as done in this paper, one can study the growth and evolution of nanostructures under various conditions.

Surface roughness control: SNBE equations are valuable for studying the evolution of surface roughness during thin film deposition. By considering stochastic fluctuations and nonlinear interactions, researchers can develop strategies to control and minimize surface roughness, which is crucial for applications such as optical coatings, semiconductor devices, and magnetic storage media.

The evolution of surface roughness during thin film deposition can be studied using stochastic nonlinear beam epitaxy (SNBE) equations that incorporate terms describing surface diffusion, deposition flux, and stochastic fluctuations.

If $h(x, t)$ represents the height of the surface at position x and time t, then the SNBE equations for studying surface roughness evolution during thin film deposition can be written as:

$$\frac{\partial h(x,t)}{\partial t} = -\nabla \cdot J(\nabla h(x,t)) + F(x,t) + \eta(x,t). \tag{6.3}$$

Equation (6.3) is an extension of (6.2). The term $F(x, t)$ can be further expanded depending on the deposition mechanism and growth conditions. In our case $F(x, t)$, can be replaced by the nonlinear term: $\lambda \nabla^2 |\nabla u(t, \mathbf{x})|^p$ and again by applying our graph formalism, a representation of the solution as well as its moments can be provided.

Optoelectronic devices: SNBE equations play a role in the design and optimization of optoelectronic devices such as light-emitting diodes (LEDs), photovoltaic cells, and semiconductor lasers. By simulating the growth process with SNBE equations, researchers can optimize device performance by controlling factors such as crystal quality, defect density, and interface roughness.

The design and optimization of optoelectronic devices such as light-emitting diodes (LEDs), photovoltaic cells, and semiconductor lasers can be facilitated by stochastic nonlinear beam epitaxy (SNBE) equations. These equations typically incorporate terms representing carrier transport, recombination, optical properties, and stochastic effects.

Let $n(x,t)$ represent the carrier concentration at position x and time t, and $E(x,t)$ represent the electric field, then the Carrier transport equation is given by:

$$\frac{\partial n(x,t)}{\partial t} = \nabla \cdot (D\nabla n(x,t)) - \frac{n(x,t)}{\tau_{\text{relax}}} + G(x,t). \tag{6.4}$$

The term $\frac{\partial n(x,t)}{\partial t}$ represents the rate of change of carrier concentration with time, $\nabla \cdot (D\nabla n(x,t))$ is the carrier diffusion term, where D is the diffusion coefficient, $-\frac{n(x,t)}{\tau_{\text{relax}}}$ is the carrier relaxation term, where τ_{relax} is the carrier relaxation time and $G(x,t)$ is the generation term representing carrier generation due to external sources or optical excitation.
The electric field $E(x,t)$ and the electrostatic potential $\Phi(x,t)$ are modeled by the Poisson equation:

$$\nabla \cdot (\varepsilon \nabla \Phi(x,t)) = -\frac{e}{\varepsilon_0}(n(x,t) - p(x,t)). \tag{6.5}$$

Here ε is the permittivity of the material, e is the elementary charge, ε_0 is the permittivity of free space and $p(x,t)$ is the hole concentration.

The rate of change of hole concentration $p(x,t)$ over time t is described by the equation:

$$\frac{\partial p(x,t)}{\partial t} = -R_{\text{rad}}(x,t) - R_{\text{non-rad}}(x,t). \tag{6.6}$$

Here $R_{\text{rad}}(x,t)$ represents the radiative recombination rate, whereas $R_{\text{non-rad}}(x,t)$ is the non-radiative recombination rate.

These equations, along with appropriate boundary conditions and material parameters, can be used to simulate the growth and performance of optoelectronic devices such as LEDs, photovoltaic cells, and semiconductor lasers. Numerical methods such as finite difference, finite element, or Monte Carlo simulations are typically employed. However, by using our approach, a power series representation is given as a solution of these equations governing optical gain, and it will provides a robust analytical tool for understanding both the rate of change and the long-term behavior of optical devices. This approach can significantly aid in the optimization of device design and performance, offering advantages in both analytical insight and computational simplicity.

7. Conclusions

The applications of stochastic nonlinear beam epitaxy equations span various areas of materials science and nanotechnology, offering valuable insights into growth processes and enabling the precise engineering of advanced materials and nanostructures for a wide range of applications.

Utilizing graph formalism, as done in this paper, can enhance these applications by providing more detailed information about the solutions, truncated moments, and the noise itself.

In materials science and nanotechnology, understanding the dynamics of surface growth processes is crucial for developing advanced materials with tailored properties. Stochastic nonlinear beam epitaxy equations are instrumental in modeling these complex phenomena, capturing the effects of randomness and nonlinearity inherent in the growth processes. This modeling approach allows

researchers to predict surface morphologies, optimize growth conditions, and design materials with specific characteristics.

Applying graph formalism to these equations provides a powerful framework for analyzing the solutions. Graphs can represent the interactions and dependencies between different components of the system, offering a clearer visualization of the growth dynamics. This method enables a systematic examination of the solution space, facilitating the identification of patterns and correlations that might be difficult to discern otherwise.

Moreover, graph formalism allows for a more precise characterization of truncated moments, which are essential for understanding the statistical properties of the system. By representing moments as nodes and their relationships as edges in a graph, researchers can effectively track the evolution of these quantities over time. This approach helps in capturing the impact of noise and fluctuations on the growth process, leading to more accurate predictions and better control over the material properties.

Additionally, graph formalism enhances the understanding of noise effects in stochastic systems. Noise plays a critical role in the growth dynamics, influencing the stability and morphology of the resulting structures. By modeling noise using graphs, it becomes possible to dissect its contributions at different stages of the growth process, providing deeper insights into how random perturbations affect the system.

In summary, the integration of graph formalism, as done in this work, into the study of stochastic nonlinear beam epitaxy equations significantly enriches the analysis by offering a detailed representation of solutions, truncated moments, and noise. This advancement not only broadens the understanding of surface growth processes but also enhances the ability to engineer advanced materials and nanostructures with precision, paving the way for innovations across various fields in materials science and nanotechnology.

Acknowledgments

This work is supported by King Fahd University of Petroleum and Minerals. The author gratefully acknowledges this support.

Conflict of interest

The authors declare that there is no conflict of interest regarding the publication of this paper.

Use of Generative-AI tools declaration

The author declares they have not used Artificial Intelligence (AI) tools in the creation of this article.

References

1. D. Blömker, C. Gugg, On the existence of solutions for amorphous molecular beam epitaxy, *Nonlinear Anal. Real*, **3** (2002), 61–73. https://doi.org/10.1016/S1468-1218(01)00013-X
2. O. Stein, M. Winkler, Amorphous molecular beam epitaxy: Global solutions and absorbing sets, *Eur. J. Appl. Math.*, **16** (2005), 767–798. https://doi.org/10.1017/S0956792505006315

3. Z. W. Lai, S. Das Sarma, Kinetic growth with surface relaxation: Continuum versus atomistic models, *Phys. Rev. Lett.*, **66** (1991), 2348. https://doi.org/10.1103/PhysRevLett.66.2348
4. J. Villain, Continuum models of crystal growth from atomic beams with and without desorption, *J. Phys. I*, **1** (1991), 19–42. https://doi.org/10.1051/jp1:1991114
5. S. Albeverio, B. Smii, Borel summation of the small time expansion of some SDE's driven by Gaussian white noise, *Asymptotic Anal.*, **114** (2019) , 211–223. http://doi.org/10.3233/ASY-191525
6. S. Albeverio, B. Smii, Asymptotic expansions for SDE's with small multiplicative noise, *Stoch. Proc. Appl.*, **125** (2015), 1009–1031. https://doi.org/10.1016/j.spa.2014.09.009
7. I. I. Gihman, A. V. Skorohod, *Stochastic differential equations*, Berlin, Heidelberg: Springer, 1972.
8. B. Øksendal, *Stochastic differential equations: An introduction with applications*, Berlin, Heidelberg: Springer, 1995. https://doi.org/10.1007/978-3-662-03185-8
9. S. Albeverio, E. Mastrogiacomo, B. Smii, Small noise asymptotic expansions for stochastic PDE's driven by dissipative nonlinearity and Lévy noise, *Stoch. Proc. Appl.*, **123** (2013), 2084–2109. https://doi.org/10.1016/j.spa.2013.01.013
10. H. Gottschalk, B. Smii, How to determine the law of the solution to a SPDE driven by a Lévy space-time noise, *J. Math. Phys.*, **48** (2007), 043303. https://doi.org/10.1063/1.2712916
11. B. Smii, D. Kroumi, A graphical representation of the truncated moment of the solution of a nonlinear SPDE, *Int. J. Anal. Appl.*, **21** (2023), 132. https://doi.org/10.28924/2291-8639-21-2023-132
12. B. Smii, Asymptotic expansion of the transition density of the semigroup associated to a SDE driven by Lévy noise, *Asymptotic Anal.*, **124** (2021), 51–68. https://doi.org/10.3233/ASY-201640
13. B. Smii, Markov random fields model and applications to image processing, *AIMS Mathematics*, **7** (2022), 4459–4471. https://doi.org/10.3934/math.2022248
14. K. K. Meng, F. Dong, T. E. Guan, *Introduction to graph theory*, World scientific Publishing Co Pte Ltd, 2007. https://doi.org/10.1142/6313
15. J. P. Serre, *Trees*, Berlin, Heidelberg: Springer, 1980. https://doi.org/10.1007/978-3-642-61856-7
16. K. I. Sato, *Lévy processes and infinitely divisible distributions*, Cambridge University Press, 1999.
17. S. Albeverio, H. Gottschalk, J. L. Wu, Convoluted generalized white noise, Schwinger functions and their continuation to Wightman functions, *Rev. Math. Phys.*, **08** (1996), 763–817. https://doi.org/10.1142/S0129055X96000287
18. M. Kardar, G. Parisi, Y. C. Zhang, Dynamic scaling of growing interfaces, *Phys. Rev. Lett.*, **56** (1986), 889. https://doi.org/10.1103/PhysRevLett.56.889

AIMS Press